

Site-dependent fate assessment in LCA: transport of heavy metals in soil

Stefanie Hellweg*, Ulrich Fischer, Thomas B. Hofstetter, Konrad Hungerbühler

Safety and Environmental Technology Group, Swiss Federal Institute of Technology Zurich, Institute for Chemical and Bioengineering, ETH Hönggerberg, HCI G129, CH-8093 Zurich, Switzerland

Received 27 August 2001; received in revised form 31 March 2003; accepted 10 October 2003

Abstract

In spite of many recent advances in the impact assessment of emissions to air, surface water, and upper-soil layers, methods for emissions to deep soil layers and the groundwater are still missing for assessment tools such as life-cycle assessment (LCA). The goal of this paper is to provide such a method for assessing the fate of heavy metals in soils. The method was developed for the emissions from slag landfills but could, in principle, also be used in other applications. Our guidelines serve to estimate the transport time needed for a heavy metal to reach the groundwater as a function of spatial parameters such as infiltration rate, macropore flow, pH value, content of organic material, and distance to the groundwater. Default values for these parameters are suggested for typical landfill sites in Switzerland. The application of the method is illustrated in three case studies of actual landfill sites in Switzerland. The results of these case studies indicate that the retardation of heavy metals varies greatly depending on the local properties of the soil considered. Moreover, it is illustrated how the suggested procedure can be integrated into existing multimedia-fate models used in LCA.

© 2003 Elsevier Ltd. All rights reserved.

Keywords: Groundwater; Heavy metals; LCA; Site- and time-dependency; Soil model

1. Introduction

Life-cycle impact assessment (LCIA) has undergone continuous improvement during the last 10 years [1–7]. However, most of these innovative approaches have been restricted to the environmental compartments fresh water, seawater, sediments, air and upper-soil layers. The groundwater compartment has rarely been considered so far. The EDIP method [4] provides the general structure for including the groundwater into the assessment, but this part of the method has not been made operational so far. Huijbregts [2] assumes that pollutant concentrations in the groundwater are equal to the concentrations in the porewater of the soil. The latter concentrations are modeled using ‘solid–water partition coefficients’ [2]. This method is well applicable,

but it neglects the strong dependence of heavy metal transport on spatial parameters.

In spite of many scientific studies about pollutant migration in soil, there is no simple generic model available for the evaluation of pollutant transport in soils. Most of the existing models such as PHREEQC [8] require detailed information, e.g., about the mineral composition of the soil, in order to calculate the speciation of metals. However, this information is not available without an elaborate analysis of the soil, which is beyond the scope of a life-cycle assessment (LCA). Moreover, the transport rates of pollutants such as heavy metals are generally small, and, thus, the deep soil layers and the groundwater are often regarded as sinks and not as safeguard subjects [9]. The omission of releases to the deep soil and the groundwater might have severe consequences in applications such as waste deposition or agricultural production, where a large share of emissions ends up in the soil (due to the deposition of heavy metal containing waste, ash, fertilizer, sludge, or compost). For instance, more than 80% of the

* Corresponding author. Tel.: +41-1-633-43-37; fax: +41-1-632-11-89.

E-mail address: hellweg@tech.chem.ethz.ch (S. Hellweg).

total environmental impact of the system waste incineration may be attributed to heavy metal emissions from slag and filter-ash landfills to deep soil layers if long-term time horizons are considered and if it is assumed that they are eventually leached to the water [10]. The vadose zone is generally regarded as a buffering zone that prevents or reduces groundwater pollution by retardation and dispersion. However, the vadose zone can also be considered as a source of groundwater pollution since heavy metals seep to the saturated zone over a long period of time [9]. These issues clearly demand a procedure suitable to assess transport velocities of pollutants in soils.

The transport of substances in the soil depends on local features of the soil and substance properties. Spatial and temporal factors are usually neglected in LCA. The resulting discrepancy between the potential impact predicted by LCA and the expected occurrence of actual impact has been heavily criticized [11–13]. In order to palliate these shortcomings, several site-dependent LCIA approaches have recently been proposed and have gained increasing acceptance among the LCA community [4,13–15]. However, none of these methods is directly applicable to the toxic emissions from landfills to deeper soil layers, because they have been designed for other impact categories or emission compartments. Fig. 1 shows how spatial parameters influence the transport of heavy metals in soil. If there is a soil layer with homogeneous low hydraulic conductivity, water might pond on top and disperse laterally to more

permeable soil or to the surface water. Vertically seeping water either flows through macropores directly to the groundwater or through the soil matrix. In the latter case, sorption processes retard heavy metal transport unless the sorption capacity of the soil is exceeded. Sorption processes depend on pollutant properties and a series of spatial parameters of the soil.

The long retardation of the heavy metals in the soil raises the question whether current emissions to the groundwater should be weighted equal to emissions in the far future. This question has recently been discussed in the LCA literature [16,17] and there are already a few studies available that generate and/or process temporal information [17–20].

The present paper proposes a site-dependent methodology that serves to estimate roughly how fast heavy metals are transported in soil. The procedure was designed for use in LCA, but could also be used in other applications such as evaluative risk assessments. First, we will discuss important processes that influence the transport of heavy metals (Section 2). Subsequently, a guideline for the estimation of transport times to the groundwater will be proposed (Section 3). Next, we apply the procedure to three landfill sites in Switzerland (Section 4) and we illustrate how the method can be used in a multimedia-box model (Section 5). Finally, we draw conclusions (Section 6).

The methodology was developed for emissions from slag landfills and will be discussed primarily in this context. Emissions from landfills might not be released

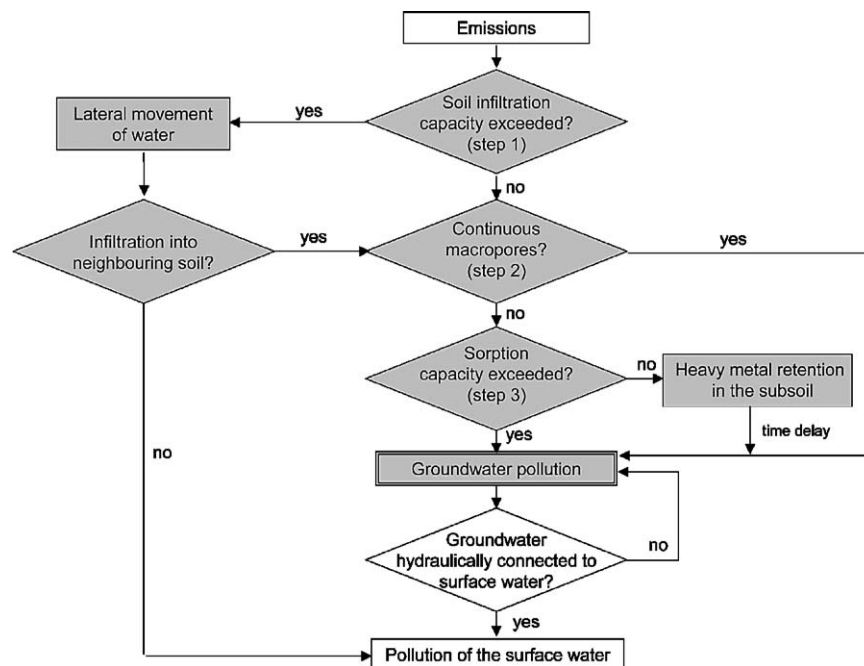


Fig. 1. Site-dependent parameters influencing the fate of heavy metal emissions from landfills. The influence of these parameters is discussed in Section 2 (theoretical background). The indication of 'steps 1–3' refers to the generic procedure proposed in Section 3.1. The shaded boxes are the pathways considered in this study.

during the first few decades after slag disposal due to modern base sealings. However, the life endurance of such technical systems is limited to less than 100 years [21–23]. Therefore, landfill leaching to the groundwater is a relevant problem in the long run, even if the landfill is of a modern standard. We assumed that once the heavy metals reach the groundwater, they leave the ‘subsoil system’ (shaded boxes in Fig. 1). The term ‘soil’ is used throughout this work, even if the underground of the landfill consists of weathered rock formations. The soil may consist of different layers as shown in the case studies of Section 4. In the present article, we define the upper-soil layer as the top 30 cm of soil [24] and the deep soil layers as the layers that are located between the upper soil and the groundwater.

2. Transport of heavy metals in soil: theoretical background

2.1. Permeability of the soil

The infiltration capacity of a soil determines whether and how much of the water or leachate can seep into the subsoil. In general, soils with a coarse soil texture (sand) permit a fast percolation, whereas soils with a fine texture (clay) retard the water flow. The information about the waterflows is often summarized in a water balance (Fig. 2). Swiss (as well as European) law requires performing an environmental impact assessment (EIA) including a hydrological–geological examination of the

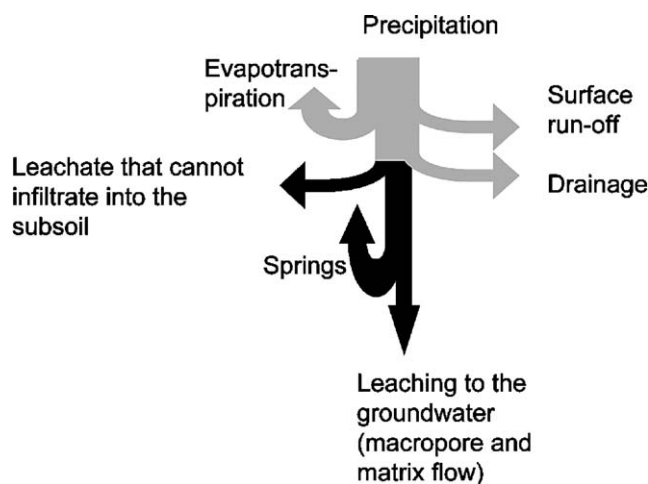


Fig. 2. Water balance: part of the rainwater evaporates or flows off on top of the surface. The remaining fraction seeps into the landfill (black arrows). If the drainage system of the landfill functions, the solute will be conducted into a water-purification plant. If the infiltration capacity of the subsoil is very low, the leachate might flow laterally away and reach the surface water. The remaining fraction seeps into the subsoil and eventually reaches the groundwater. Springs transport part of the solute to the surface again. In the water balance, the widths of the arrows indicate the rough proportions of flows.

site before the construction of a landfill [25]. The EIA report either contains the whole water balance or information on the rate of new groundwater formation and/or hydraulic conductivity, precipitation, evapotranspiration, and surface run-off. The hydraulic soil conductivity is an indicator of how fast water can flow through soil. The rate of new groundwater formation can (in most cases) be taken from the EIA report or a hydrologic atlas. It generally varies between 30% and 50% of the amount of annual precipitation at well-permeable sites [26].

2.2. Continuous macropores (preferential flow)

Macropore flow refers to transport of water and solutes in distinct flow channels, which can be thought of as separated from the soil matrix [27]. Macropores may be fractures or cracks (temporary shrinkage cracks, permanent structural cracks, soil layering, etc.), worm holes, or root channels. They can be continuous for distances of several meters [28]. The fraction of macropore flow in soils can be high reaching up to more than 90% of the total flow. Since continuous macropores bypass the soil matrix, sorption processes are of minor importance for the transport of heavy metals [27]. As a result, heavy metals have been found in deep soil layers [29–31]. Richards et al. [32] and Cambreco et al. [33] list a large amount of studies that were unable to establish mass balances when investigating metal mobility in soils. A possible explanation is accelerated transport through macropores [32].

It is often difficult to estimate the fractions of water that are subject to macropore flow, interrupted macropore flow, and inhomogeneous flow through the soil matrix [33]. Moreover, the number of continuous macropores in soils varies in time and space [28,34]. This could be taken as an argument against trying to determine the macropore flow. However, because we are interested in large landfill areas and long time horizons, a reasonable average estimation of the flow through continuous macropores can be sufficient. Diffusion from continuous macropores into the soil matrix along the flow channels is small [34,35] and, therefore, neglected in the present work.

The extent of macropore flow depends on the soil texture and other spatial parameters, the most important of which are listed in the first column of Table 1. The second column indicates the influence of these parameters on macropore flow if their value increases. In the third column, the temporal variability of the corresponding parameter is characterized. An explanation of the governing mechanisms is given in the last column. Occasionally, estimates of the fraction of macropore flow can be found in the EIA report of the landfill. However, in many cases, the few soil samples taken prevent inhomogeneities from being recognized

Table 1

Site-dependent parameters influencing macropore flow in soils. The second column indicates the influence of an increase of the parameter values of column 1 on macropore flow (\uparrow = increase of macropore flow, \downarrow = decrease of macropore flow). In the third column, the temporal variability of the corresponding parameter is characterized. An explanation of the governing mechanisms is given in the last column

Site-dependent parameter ^a	Influence on macropore flow	Temporal variability	Explanation
Soil texture (grain size)	\downarrow	Small	Under comparable conditions, relative macropore flow is largest for the finest textured medium [35,65,66]. Therefore, macropore flow has normally a higher share in clay soils than in silt or sand soils.
Depth in soil	\downarrow	Small	The number of continuous macropores decreases with depth [41]. Some of the reasons are the absence of plants and earthworms in deep soil/rock layers, and higher pressure.
Thickness of the soil layer	\downarrow	Small	Thin soil layers are more vulnerable than thick ones [67] due to the higher probability of continuous macropores.
Water content of the soil and infiltration rate	(\downarrow), \uparrow	High	Macropore flow might increase with soil moisture and rain intensity [65,68]. For instance, infiltration into dry soil might fill up voids in the matrix first. Macropore flow is reduced to directly infiltrating water then. When the infiltration capacity of the soil matrix is exceeded, water passes to the macropores [69]. Moreover, macropore channels have variable width and continuity depending on rain intensities and water saturation. High infiltration rates and ponding increase the continuity of macropores by activating laterally interconnecting macropores [34]. However, in dry soils shrinkage cracks might contribute to increase the macropore flow (e.g., [70]).

^a Only the most common (and important) parameters are mentioned. Effects like the formation of macropores by precipitation mechanisms [45] or funneling effects by low-permeable soil layers [71] are not considered.

[22]. In Section 3.1, a simplified procedure for estimating the potential share of macropore flow will be proposed.

2.3. Sorption (matrix flow)

Adsorption, complexation, and precipitation influence the transport velocity of heavy metals in soils. These processes depend on spatially variable parameters and on the speciation of the metal. However, the speciation of metals depends on many parameters (such as the mineral composition of the soil) that are generally not known in the framework of an LCA. Therefore, simplifications need to be made. In the current work, we distinguish between three types of heavy metal species:

1. metals that form oxyanions such as MoO_4^{2-} and SbO_4^{2-} ;
2. metal cations (especially hydroxo-complexes) that may be sorbed to surface sites;
3. metal organic complexes.

Heavy metal oxyanions such as MoO_4^{2-} and SbO_4^{2-} (type 1) are primarily leached from landfills during the first centuries after disposal when the pH value is high. Heavy metal oxyanions are mostly specifically adsorbed to Al- and Fe-oxides as well as clay minerals. Specific adsorption decreases with an increase in pH and a decrease in the anion concentration in the solution [36]. In Switzerland, soils generally contain much calcite and the pH value is consequently neutral to basic. Anion adsorption is therefore limited and transport to the groundwater fast. In the current work, we assume that transport times for metal anion species are negligible.

The focus of the current work lies on the transport of heavy metal cations (types 2 and 3). The most important parameters determining transport velocities are listed in the first column of Table 2 following the same format as Table 1. Adsorption increases with the concentration of dissolved heavy metals in the leachate as long as the corresponding surface sites are available. Heavy metal ions compete for exchange sites at the soil matrix. The preferential adsorption of heavy metals strongly depends on the metal concentration and the type of interaction with the solid surface. Some heavy metal cations like Cu^{2+} and Pb^{2+} may form complexes with dissolved organic acids in the landfill. Whether the subsoil can retain these organic complexes depends on the content of organic matter. Dissolved organic complexes have been observed to directly penetrate to the groundwater [24].

2.4. Groundwater

The location of the groundwater table and the groundwater flow (volume of groundwater, flow paths, and velocities) depends on local conditions. The EIA report usually contains (uncertain) information on the

groundwater table and the groundwater flow. The location of the groundwater is an important parameter to consider when estimating the transport time needed for heavy metals to penetrate through the soil. One reason is that the fraction of macropore flow decreases with an increase in transport distance. Another reason is that the transport time for the heavy metals passing through the soil matrix increases with distance. In the case studies of Section 4, transport of heavy metals in the groundwater is fast in comparison to transport in the landfill or soil. Therefore, we assumed that transport within the groundwater is not a limiting factor when estimating the transport time. However, the groundwater flow is important with respect to the assessment of pollutant concentrations in the groundwater.

2.5. Further spatial aspects

Several spatial aspects have not been mentioned above and are neglected in this paper. For instance, future changes of the groundwater table were not considered. Similarly, changes in climate leading to a change in precipitation rate and vegetation (e.g., due to the greenhouse effect) and exceptional events like earthquakes were not taken into account.

3. Site-dependent fate assessment of heavy metal cations in soil

Site-specific properties of the soil determine the ultimate fate and temporal dispersion of heavy metals in the soil. The logic tree method will be used to display these properties (Fig. 3). Logic trees are decision-supporting instruments in which uncertain events or states of nature are considered. The branches indicate possible values of site-dependent parameters that are mutually exclusive. A (conditional) probability is assigned to each branch. The sum of probabilities of every node is 100%. Each path leading to a leaf represents a scenario [37].

Logic trees are constructed for every soil layer thicker than 30 cm (or at least for those soil layers that have the strongest effect on heavy metal retention). Default values for Swiss landfill sites are suggested for the case that no specific data are available. These default values refer to new landfill sites that meet the requirements of the current legislation. At old sites, other values would be more suitable (see also case studies in Sections 4.1 and 4.2). Fig. 3 shows the complete logic tree that will be explained step by step in the following Section 3.1. After explaining the different steps of the method, we show how this approach can be used in multimedia-box models that are often applied in LCIA (Section 3.2).

Table 2

Parameters influencing the mobility of heavy metal cations in normally polluted soils [24,72]. The second column indicates the influence of an increase of the parameter values of column 1 on the mobility of heavy metals (\uparrow = increase, \downarrow = decrease). In the third column, the temporal variability of the corresponding parameter is characterized. An explanation of the governing mechanisms is given in the last column

Site-dependent parameter	Influence	Temporal variability	Governing mechanisms
pH value	\downarrow	In buffered systems small, otherwise high	Adsorption: The specific adsorption of metals (stronger than unspecific sorption) increases and the mobility is reduced if the pH is high; this is especially the case for Cd^{2+} , Ni^{2+} , Zn^{2+} , Cu^{2+} , and Pb^{2+} because they form hydroxo complexes, which adsorb to sesqui-oxides (hydroxylized surfaces of Fe-, Al- and Mn-oxides). Organic metal complexes with a reduced mobility are formed above a certain pH. However, some metals like Pb^{2+} and Cu^{2+} might form mobile soluble organic complexes. Under slightly basic conditions, the solubility of heavy metal cations is limited [46]. Immobile metal sulfides might be formed under reducing conditions. A low pH facilitates the formation of metal sulfides.
Inclination of metal to form hydroxo-complexes	\downarrow	–	See also above line 'pH value'. The hydroxo complexes of metals are especially well sorbed to sesqui-oxides. Therefore, sorption increases with an increasing affiliation of metals to form hydroxo complexes.
Content of sesqui-oxides and clay	\downarrow	Small	See also above line 'pH value'. The influence of Fe(II/III)- and Mn(III/IV)-oxides on metal adsorption is larger than that of clay minerals and organic material. However, the occurrence of these sesqui-oxides is correlated with the clay content.
Content of organic material	\downarrow , (\uparrow)	Medium	The mobility of organic metal complexes is generally limited. However, dissolved organic metal complexes might be subject to fast transport.
Redox potential	\uparrow	High	Immobile metal sulfides might be formed under reducing conditions.
Influence of metals on each other	\uparrow , \downarrow		The presence of other heavy metals might influence the mobility. For instance, Cd^{2+} mobility can be enhanced by high concentrations of Pb^{2+} .

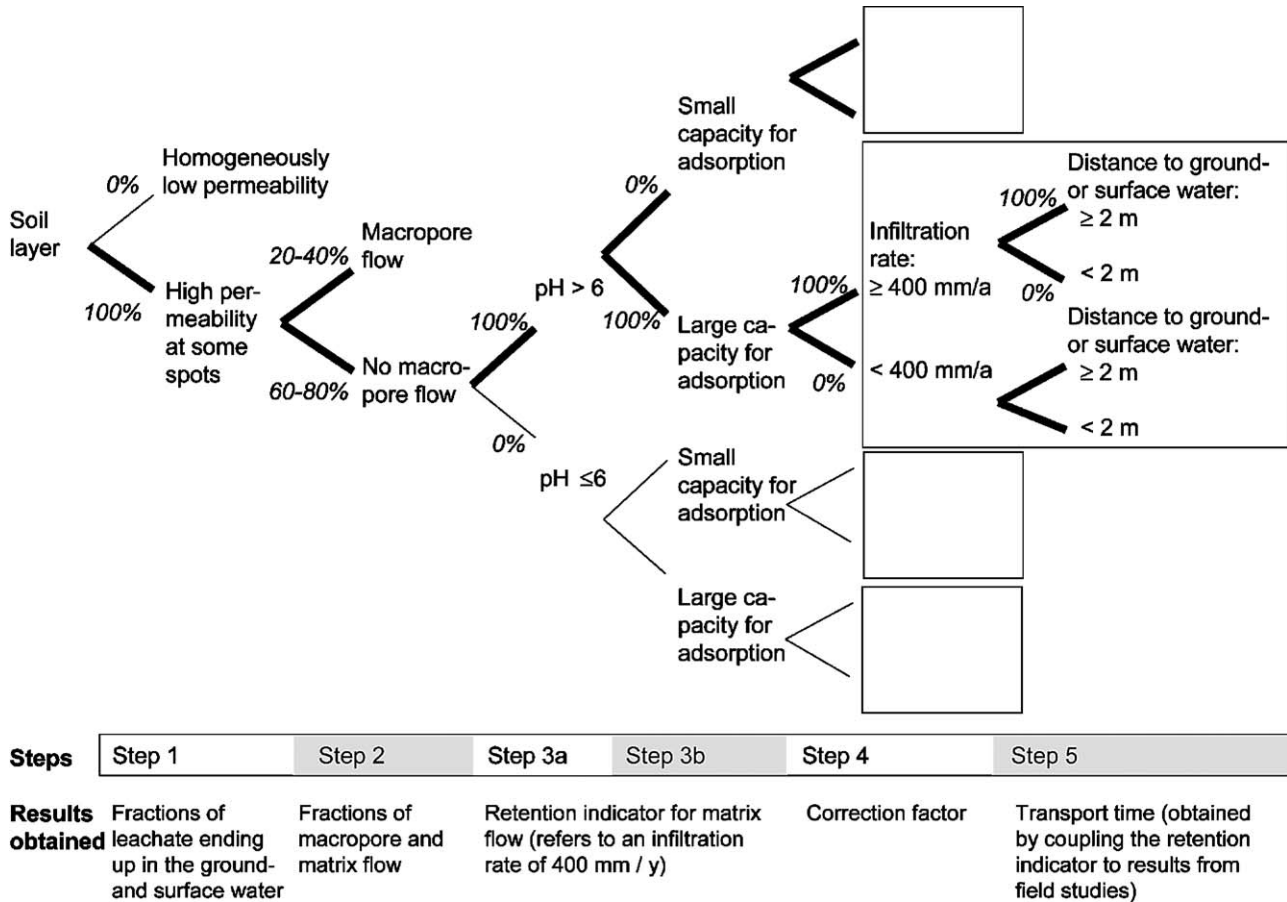


Fig. 3. Logic tree for transport through a soil layer. The pathways printed in bold are typical scenarios for current Swiss landfill sites (old and new standard). The branches carrying probabilities greater than 0% are suggested as default values for typical new landfill sites in Switzerland fulfilling the standards of the TVA [39] (with the exception of the hydraulic conductivity, see text). The contents of the boxes are identical. The indication of 'steps 1–5' refers to the generic procedure proposed in Section 3.

3.1. Procedure for estimating transport times of heavy metals in soils

3.1.1. Step 1: permeability of the soil layer

If a soil layer has a homogeneously low hydraulic conductivity of $k < 10^{-7}$ m/s (upper branch of step 1 in Fig. 3), water will probably pond on top [38]. Laterally moving water may contaminate the surface water so that the logic tree should be constructed for the water-conducting layer. If the examined soil layer is already the top layer, it is assumed that the leachate is emitted to the surface water right away. In case of a hydraulic conductivity of $k > 10^{-7}$ m/s (lower branch in Fig. 3) proceed with step 2.

3.1.1.1. Default values for soil permeability in Switzerland. The Swiss Technical Guideline Waste (Technische Verordnung Abfall, TVA) [39] rules that landfill sites should be constructed over a homogeneous soil layer with a thickness of 7 m and a hydraulic conductivity of $k < 10^{-7}$ m/s. However, sites with such a

homogeneously low hydraulic conductivity do not exist in Switzerland [38]. Therefore, the default value for Swiss landfills is 0% for the upper branch and 100% for the lower branch.

3.1.2. Step 2: continuous macropores

Emissions flowing through macropores might pass directly and unbuffered to the groundwater. It is assumed that macropore flow is quick and that the transport time is negligible. Therefore, the transport time of the fraction of macropore flow is less than 1 year (upper branch of step 2 in Fig. 3). If the water passes through the soil matrix (lower branch), proceed with step 3a.

The fraction of macropore flow is difficult to anticipate. Some indications are the parameters mentioned in Table 1 and the results from experimental studies (Table 3). In some situations, a comparison of the hydraulic conductivity measured in field experiments and the hydraulic conductivity measured in the

Table 3
 Fraction of macropore flow compared to the total flow in silty and clayey soils (overview of experimental studies or simulations based on experiments)

Soil type	Soil texture	Depth/thickness	Infiltration rate/soil moisture	Fraction of macropore flow	Ref.
Silty soil	Composition: 8–18% sand, 47–74% silt, 18–35% clay	50 cm	Infiltration rate: 0.12, 0.6, and 3 mm/min; in the latter two cases ponding	32–43%	Ref.
	Silty loam (coarse loamy, mixed, mesic Psammentic Hapludalf)	35 cm	Infiltration rate: 30 mm/day	40–50%	[42]
	Fine-silty, mixed, mesic typic Fluvaquent (36% silt, 31% clay)	20 cm	Infiltration rate: 0.03 and 0.06 mm/min for 50 and 25 min; pressure head $h = -1000$ and -200 cm	45% at $h = -1000$ cm, 70% at $h = -200$ cm	[33]
	Sandy loam (24–26% sand, 55–56% silt, 15–20% clay)	1 m	Saturated conditions	More than 99%	[73]
Clayey soil	Light to medium-heavy clay (31–44% clay content)	1 m	High soil moisture (groundwater table: 0.5–1.4 m)	41%	[74]
	Clay (often > 50% smectites)	43 cm	Soil saturation between 35% and 95%	35%	[75]
	Very fine clayey, mixed illitic–montmorillonitic, mesic typic Fluvaquent (52–69% < 2 μ m)	0.77 cm (tile drains)	Natural precipitation between 0 and 23 mm/day; soil moisture between 33% and 60%	0–80% depending on the rain intensity and soil moisture	[76]
	Heavy clay soil	1.8 m	Natural precipitation (infiltration rate 330 mm/year)	30–40%	[70]
	Very fine clayey, mixed illitic–montmorillonitic, mesic typic Fluvaquent (51–60% clay)	1.2–1.4 m (tile drain)	Natural precipitation and soil moisture	Large fraction, under dry soil conditions all transport	[67]
	Clay loam (25–35% clay) and clay (50–100% clay)	20 cm	Rain intensity: 250 mm/day, initial pressure head: 25 kPa	64% (clay loam), 79% (clay)	[77] and [78]

laboratory (homogeneous column tests) may provide a rough estimate of the fraction of macropore flow.

3.1.2.1. Default values for macropore flow in different soils. In many experimental studies, piston flow could be observed in soils with a high content of sand (sand content higher than 75%) [27,40,41]. Piston flow is defined here as a uniform flow as opposed to preferential flow. Therefore, the probability of macropores could be assumed to be close to 0% for sandy soil layers. Macropore flow in silty and clayey soils, on the contrary, is often considerable [34,41,42]. Table 3 shows the results of some experimental studies. Considering the results of Table 3, we suggest a default value of 30–70% macropore flow for silty soil layers thinner than 1 m (the value for the sandy loam in the 4th line of Table 3 is ignored, since we do not assume that the soil will be completely saturated) and 35–80% for clayey soil layers. These estimates should be adapted according to Table 1, if the soil layer is thicker than 1 m or if the infiltration rate or soil moisture varies considerably from the values given in Table 3.

3.1.2.2. Default values for macropore flow in Switzerland. The TVA requires a subsoil of low permeability. Therefore, new landfills are usually built on clay layers that provide favorable conditions for macropore flow. These layers should be thick (7 m according to the TVA), which lowers the probability of continuous pores. Considering the above and Tables 1 and 3, we suggest a default value of 20–40% for the fraction of macropore flow.

3.1.3. Step 3a: sorption (as a function of pH)

Adsorption and precipitation processes as well as the formation of metal organic complexes depend on the pH value of the soil matrix (Table 2). Under neutral and basic conditions, the mobility of heavy metals is minimal [24] (step 3a in Fig. 3). In the present procedure, a retention indicator is determined in function of the pH according to Table 4. The retention indicator serves for a classification of the mobility of the heavy metals in soils. The higher the value of the retention indicator, the more the heavy metal of concern is retarded.

3.1.3.1. Default value for the pH value in Swiss soils. In Switzerland, soils at suitable sites for landfills contain much calcite [43]. Thus, the pH value is always slightly basic (pH ~8).

3.1.4. Step 3b: sorption due to enhanced content of sesqui-oxides and formation of organic metal complexes

Heavy metal adsorption increases with the content of sesqui-oxides in the soil (Table 2). The presence of all

sesqui-oxides, but Fe-oxides, is correlated with the content of clay [24]. Further, an enhanced content of organic material may also delay heavy metal transport (Table 2). Therefore, supplements to the retention indicator may be given if the content of sesqui-oxides and/or organic material is high in the soil (Table 5).

The cation exchange capacity (CEC) quantifies the number of exchangeable cations in a soil matrix [36] and is therefore an indicator of how many cations can be adsorbed. The values for the CEC of different clays are given in Table 6.

The leaching water from a slag landfill typically contains about 285 mmol_c Ca²⁺, Cd²⁺, Zn²⁺, Pb²⁺, and Cu²⁺ per year and m² as long as calcite is present in the landfill (the index c in the unit mmol_c indicates charge) [44]. A comparison between the CEC and the cation content of the leachate indicates whether or not heavy metals might be retarded considerably by adsorption. For instance, opalinus clay in Switzerland (20% smectite, 15% illite, 10% chlorite, 10% kaolinite) has a CEC of 120 mmol_c/kg [45] or 180,000 mmol_c/m³ (the storage density of soil is approximately 1500 kg/m³ [38]). Therefore, the CEC of 1 m³ opalinus clay would be exceeded after about 630 years assuming that all cations of the leachate (285 mmol_c) are adsorbed. Exceeding the CEC does not mean that cations are no longer adsorbed. Cation exchange continues to take place. However, adsorption is supposed to be limited in this case.

If the sorption capacity is small in comparison to the cation content of the leachate, supplements according to Table 5 should not be granted. The final retention indicator (RI_{final}) can be calculated according to Eq. (1a) if the CEC is small and according to Eq. (1b) if the CEC is large.

$$RI_{\text{final}} = RI_{\text{Table 4}} \quad (1a)$$

$$RI_{\text{final}} = RI_{\text{Table 4}} + \text{Supplements}_{\text{Table 5A,B,C}} [-] \quad (1b)$$

3.1.4.1. Default values for the cation exchange capacity and the content of organic material at Swiss landfill sites. The TVA [39] requires a clay layer of 7 m below the landfill. If these requirements are met, the CEC would be exceeded after about 5600 years (assuming an average CEC of 120 mmol_c/kg). This time period is certainly not negligible. It is assumed that the clay content ranges from 25% to 45%. If the TVA is not met with respect to the clay layer, no supplements should be granted. For Fe-oxides, it is recommended not to give supplements to be on the safe side (we do not define a default value for Switzerland). Concerning the content of organic material, we suggest a default value of less than 2% organic material, which is justified for deeper soil layers [43].

Table 4

Retention indicators (RI) for several metals and pH values (values in roman font from [24]^a). The retention indicator takes into account the inclination of metals to form hydroxides and the dependency on the pH value (see Table 2). The retention indicators may be increased according to Table 5 in order to consider other influencing factors such as an enhanced content of clay, sesqui-oxides, and organic material in the soil

pH value	3.5	4	4.5	5	5.5	6	6.5	7	7.5
Cd ²⁺	1	1.5	2	3	3.5	4	4.5	5	5.5
Zn ²⁺ , Ni ²⁺	1.5	2	3	3.5	4	4.5	5	5.5	6
Cu ²⁺ , Cr ³⁺	2	3	4	4.5	5	5.5	6	6.5	7
Pb ²⁺ , Hg ²⁺	3	4	5	6	7	8	9	10	11

^a In DVWK [24], the maximal retention indicator is limited to a value of 5. Heavy metals are considered as largely immobile in such soils. However, in contrast to the present study, uncontaminated soils and short-term time horizons were considered in the original study [24]. In the present work, no upper limit is set for the retention indicator (see italicized values in Table 4). The retention indicator rises with an increase of the pH value because of two reasons: First, the cation exchange capacity rises with an increase in pH due to an enhanced dissociation of H⁺-ions of surface bound OH⁻ and OH₂ groups (leading to an increase of surface sites) [36]. Second, more heavy metal carbonates and (hydr)-oxides generally precipitate when the pH rises to a neutral or slightly basic value [46]. The values in italics are an uncertain guess. For instance, dissolved organic complexes and colloid transport could also increase the mobility at high pH values [38]. However, the experimental results presented in Fig. 4 are in reasonable accordance with our estimates.

3.1.5. Step 4: matrix infiltration rate

The matrix infiltration rate (Eq. (2)) influences the transport velocity of heavy metals in soil. If the infiltration rate is small, transport of heavy metals will also be limited.

$$IR_{\text{matrix}} = \text{TL} - \text{SF} - IR_{\text{macropore}} \text{ (mm/year)} \quad (2)$$

where IR_{matrix} is the matrix infiltration rate (mm/year), TL the total leachate (mm/year), SF the leachate that cannot infiltrate into the subsoil (surface flow) (mm/year), and $IR_{\text{macropore}}$ the macropore flow in the subsoil (mm/year). The total leachate TL is the amount of precipitation minus evapotranspiration, surface run-off, and possibly drainage. At a landfill site, it represents the leachate from the landfill to the subsoil (black arrows in Fig. 2).

The retention indicator calculated in step 3 (Tables 4 and 5) referred to an infiltration rate of 400 mm/year. If the matrix infiltration rate is smaller than 400 mm/year, the transport time of heavy metals to the groundwater will increase. We define the correction factor I as the ratio of this infiltration rate of 400 mm/year and the matrix infiltration rate at the site under study (Eq. (3)).

This factor is necessary for the estimation of the transport time of heavy metals to the groundwater in step 5.

$$I = \frac{400 \text{ mm/year}}{IR_{\text{matrix}}} [-] \quad (3)$$

3.1.5.1. Default value for the matrix infiltration rate in Switzerland. At a typical site in Switzerland, $TF_{\text{landfill}} = 400$ mm rainwater per year seep into the landfill [46,47]. We assume that the landfill leachate can infiltrate completely into the subsoil ($SF = 0$). The fraction of macropore flow in the subsoil was set to 20–40% as default value (step 2). This gives a value of 1.25–1.67 for the factor I (Eqs. (2) and (3)).

3.1.6. Step 5: estimation of the transport rate and the time to reach the groundwater

The time needed to transport a heavy metal to the groundwater is the ratio of the distance to the groundwater and the transport rate. We assume that the transport rate is a function of the retention indicator

Table 5

Supplements to the retention indicator (Eq. (1b)) for (A) enhanced content of clay (correlated with content of sesqui-oxides, the supplement should be reduced by 0.5 for each 25 weight percent gravel or stones), (B) enhanced content of Fe-oxide, and (C) enhanced content of organic material [24]

(A) Clay content	5–15%	15–25%	25–45%	>45%
Zn ²⁺ , Cu ²⁺	0	0.5	0.5	1
Pb ²⁺ , Cr ³⁺ , Hg ²⁺	0.5	0.5	1	1.5
(B) Fe-oxide (chroma:value ^a)	1–1.5	>1.5		
Cd ²⁺ , Zn ²⁺ , Ni ²⁺	0.5	1		
Cu ²⁺	1	1.5		
Pb ²⁺ , Cr ³⁺ , Hg ²⁺	1.5	2		
(C) Organic material	2–8%	8–15%	>15%	
Zn ²⁺	0	0.5	0.5	
Ni ²⁺	0.5	1	1	
Cd ²⁺	0.5	1	1.5	
Cu ²⁺ , Pb ²⁺ , Cr ³⁺ , Hg ²⁺	1	1.5	2	

^a Chroma: intensity of color. Value: brightness. The values can be deduced from the Munsell charts [79].

Table 6
Typical values for the potential cation exchange capacity (CEC) of clay minerals [36]

Clay mineral	CEC (mmol _c /kg)
Kaolinite, halloysite	30–150
Illite	200–500
Vermiculite	1500–2000
Smectite	700–1300
Chlorite	100–400
Allophane	100–500

calculated in step 3. In order to quantify this relationship between transport rate and retention indicator, results about the transport rates in experimental studies are required. Because transport of heavy metals in soil is slow, studies with time scales of a few decades to a few centuries are needed. There are only a few case studies of historical industrial sites that meet this requirement. For instance, Maskall et al. [30,48] investigated smelting sites ranging in age between 220 and 1900 years. On these sites, Pb²⁺ and Zn²⁺ have been transported various meters into the soil. Such observations are impossible in short-term laboratory tests. On the other hand, uncertainties are large due to missing information. For instance, there is no possibility of mass balance calculations since the information on the initial emission quantities is not available.

In Fig. 4, the transport rates found in field studies for Pb²⁺ migration [30,48] have been combined with the retention indicators of step 3 (Sections 3.1.3 and 3.1.4). The calculation of the retention indicators for the given sites is summarized in Table 7. Since the field sites were heavily polluted, no supplements were given in step 3b.

The results of Fig. 4 confirm that transport rates decrease with an increasing retention indicator (see linear regression trend line, $R^2 = 0.64$). The transport rates from Fig. 4 will be used for an estimation of the

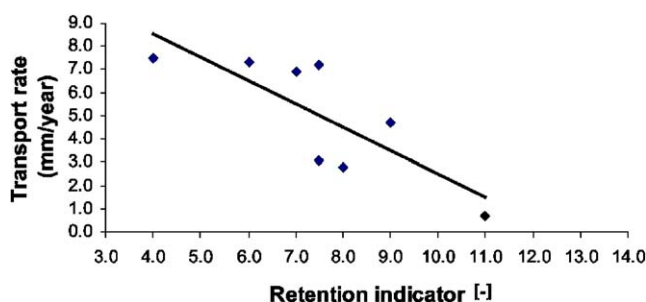


Fig. 4. Transport rates of Pb²⁺ migration observed in field studies [30,48] on heavily polluted sites as a function of the retention indicator (steps 3–5 in Section 3, infiltration rate >400 mm/year). The transport rate was calculated according to the following formula: (depth of deepest soil sample with enhanced Pb²⁺ content)/(time span after emission). These experimental results for Pb²⁺ were used for all heavy metals since the retention indicator considers the individual transport properties of the heavy metals. The line in the graph was established by linear regression.

transport time of heavy metals needed to reach the groundwater. Since these transport rates were measured at an infiltration rate higher than 400 mm/year, we need to adapt the value for the transport rate if the infiltration rate varies from this value. This correction is done with the factor I (Eq. (3)) calculated in step 4. Using this information, we can approximate the transport time using Eq. (4):

$$t = \frac{I \times D}{tr} (\text{year}) \quad (4)$$

where t is the time that is needed to reach the groundwater (matrix flow) (year), I the correction factor calculated in step 4 [–] (Eq. (3)), D the distance of the emission source to the groundwater (m), and tr the transport rate (m/year) (Fig. 4).

3.1.6.1. *Default values for the distance to the groundwater in Switzerland.* Although there are also landfill sites with a shallow groundwater table, we assume as default value that the distance to the groundwater is larger than 2 m.

3.1.7. Summary of default values for landfill sites in Switzerland

In Fig. 3, the default values suggested in steps 1–5 were assigned to the corresponding branches of the composed logic tree. About 20–40% of the metals are supposed to directly reach the groundwater without temporal retardation (macropore flow). Concerning the remaining 60–80%, the default values for the retention indicators and corresponding transport rates for Switzerland are presented in Table 8.

3.2. A box-model for transfer of heavy metals from soil to ground- and surface water

The above procedure may be directly used to obtain the information, at which point in time emissions to the groundwater are to be expected. However, in present LCAs, such consideration of temporal information is still the exception (see Section 6). Many new-generation LCIA methods consider the fate of pollutants by applying multimedia models with a multiple pathway exposure model [1,2,49]. These models consider degradation and transfer of pollutants between environmental compartments [50]. With such models, concentration increases of a pollutant in the different environmental compartments that result from an emission as well as average daily doses to humans can be calculated. The compartments are assumed to be well mixed and concentrations are therefore uniform. The inflowing emission flux may be maintained constant until steady-state concentrations are reached in the environment ('level III model'). These level III multicompartment models are usually used by current LCIA methods

Table 7

Calculation of retention indicator for transport of Pb^{2+} at historical smelting sites [30,48] (heavily polluted soils, infiltration rate ≥ 400 mm/year). If two values were calculated (different soil layers), the highest value was used (printed in italics)

Site name	Time since initial contamination (year)	pH	Retention indicator RI [-] (step 3a)
Cupula A	222	Sand layer: 5.9 Clay layer: 4.3	Sand: 8 Clay: 4.5
Cupula B	240	5.8	7.5
Bole A	567	3.9	4
Bole B	567	Sand layer: 5.8 Clay layer: 5.3	Sand: 7.5 Clay: 6.5
Bole C	600	5.4	7
Bole D	600	5.1	6
Roman A	1900	Sand layer: 7 Clay layer: 7.5	Sand: 10 Clay: 11
Roman B	1900	6.6	9

[1,2,49]. By contrast, ‘level IV models’ allow a dynamic modeling of concentration increases in the environment as a function of time (for an example see [51]).

In a similar way, we used the procedure described in Section 3.1 to model the transfer of metals from the upper soil to the deep soil layers and to the groundwater and fresh water (black arrows in Fig. 5). Since we apply the model to heavy metals, degradation is not of relevance. To maintain the model simple, we focus on the exposure of humans by drinking groundwater and disregard other exposure pathways and some compartments (e.g., air). These neglected compartments and exposure pathways have already been considered by previous methods (e.g., USES-LCA [2]). Our approach could theoretically be integrated into these existing models (Section 5).

For illustration purposes, we calculated concentration increases of Cd as a consequence of an emission inflow at a fictitious European site. Several assumptions and parameter definitions had to be made (Tables 8 and

9). We assumed that the total groundwater volume remains constant in the system. Therefore, the outflow volume of water (e.g., outflow via springs) is equal to the rate of new groundwater formation. The rate of new groundwater formation generally varies between 30% and 50% of the amount of annual precipitation at well-permeable sites with groundwater reservoirs beneath [26]. Since only a fraction of the European surface can be classified as well permeable, the rate of new groundwater formation was assumed to be 5% (in analogy to [52]). We assumed one scenario with polluted macropore flow and one scenario with non-polluted macropore flow. The former scenario should be used if the percolate is contaminated, e.g., in case of landfill emissions, while the latter scenario is more suitable if metal concentrations in the leachate are low. If the leachate is not contaminated, mainly unpolluted water is transported through the macropores to the groundwater. Further, we assumed that the total volume of groundwater is about 10 times the volume of annual new groundwater formation. The emission inflow was defined to be 1000 kg Cd/year to the upper-soil compartment (for dimensions of the soil compartment, see Table 9).

The result of the model calculations was predicted concentration increases in the upper soil, the groundwater, and the outflow to the surface water at steady state and after certain time-cuts (as done in [2,51]). From there, predicted daily intakes (PDI) and risk ratios (risk ratio = PDI/HLV, HLV is the human limit value) were calculated as done in [2]. These risk ratios can be used in the characterization step of LCIA [2].

4. Application of the procedure in case studies about landfills in Switzerland

Although landfills have a relatively short history in comparison to their emission period, some severe events

Table 8

Retention indicators, estimated transport rates of pollutant fronts, and transport times to reach the groundwater (only matrix flow) for heavy metal cations at typical new landfill sites in Switzerland and at a model site in Europe

	Typical landfill site in Switzerland						Model soil in Europe	
	Cd^{2+}	Ni^{2+}	Zn^{2+}	Cu^{2+}	Cr^{3+}	Pb^{2+} , Hg^{2+}	Cd^{2+} upper soil	Cd^{2+} deep soil
Retention indicator [-]	5.5	6.0	6.5	7.5	8	12	5.5 ^a	5 ^a
Transport rate t_r (mm/year) (Fig. 4) ^b	7	6.5	6.0	5	4.5	0.5	7	7.5
Correction factor I [-] (Eq. (3)) ^c	1.25–1.67	1.25–1.67	1.25–1.67	1.25–1.67	1.25–1.67	1.25–1.67	16	16
Distance to the groundwater or thickness of soil layer (m)	2–10	2–10	2–10	2–10	2–10	2–10	0.3	0.2–4.7
Time to reach the groundwater/next soil layer (year) (rounded to two significant digits)	360–2400	380–2600	420–2800	500–3300	560–3700	5000–33,000	690	430–10,000

^a It was assumed that the pH value is neutral and that there is an enhanced content of organic material (2–8%) in the upper-soil layer.

^b Refers to an infiltration rate of 400 mm/year.

^c At typical landfill sites in Switzerland, the matrix infiltration rate is between 240 and 320 mm/year. For the fictitious soil in Europe, we assumed a matrix infiltration rate of 25 mm/year (see text and Table 9).

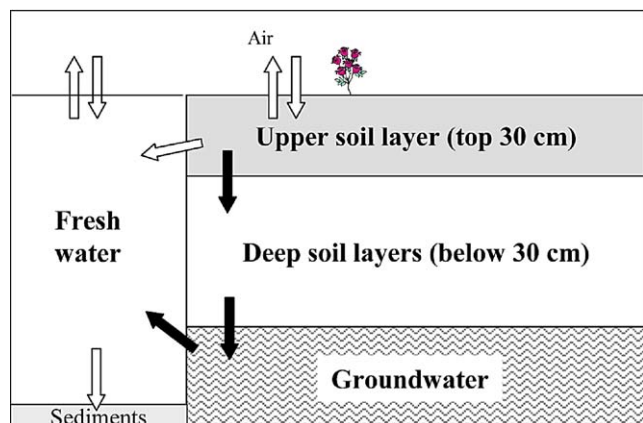


Fig. 5. Simplified multimedia model considering an upper-soil and deep-soil compartment as well as the groundwater. In the model calculations, transfer from the soil to the groundwater and from there to the fresh water is considered (black arrows). Exposure of humans takes place via ingestion of drinking water from groundwater.

with heavy groundwater pollution have already occurred in the past two decades. The landfills Kölliken and Bärengraben are two examples where preferential transport of pollutants has been observed and where the subsoil has been heavily polluted [38,53]. In the following, three Swiss case studies are presented. Since some of the landfill operators wished to remain anonymous, we refer to the sites as site A, B, and C.

4.1. Case study: site A

On site A, there are two old landfills without technical barrier systems. Fig. 6 shows the geological layers and the water balance. The bedrock consists of limestone. It has open fractures and cracks and maintains a well-communicating groundwater system. Leaching water could possibly reach a drinking water reservoir [54,55]. Sorption in the karst is limited because of fast preferential flow. However, it is likely that concentrations are considerably diluted. Above the

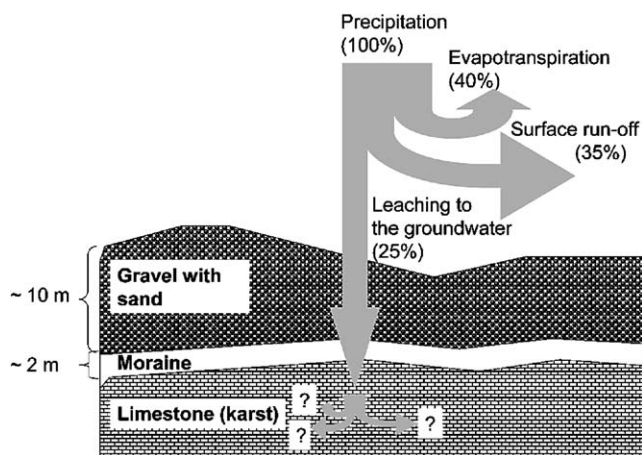


Fig. 6. Water balance at site A [55]: a large fraction of the rainwater (75%) evaporates or flows off on top of the soil surface. The remaining fraction (25%) seeps into the landfill and from there to the subsoil and groundwater. The flow paths of the groundwater are not known.

bedrock, there is a moraine layer (clayey, silty gravel with sand). The moraine has only a limited function as hydraulic barrier due to large inhomogeneities and because of its inclination. The top layer (gravel with sand) is permeable ($k < 10^{-4}$ m/s) [54,55].

The upper-soil layer may have macropores due to the large content of gravel. Macropores in the moraine layer also exist because this soil layer is not homogeneous, fractured, and inclined. We estimate the macropore flow to be about 50% (considering the proposed default values of Section 3). The heavy metals of the remaining 50% matrix flow will be retarded due to sorption processes. The pH value is between 7 and 8 in all soil layers due to the presence of calcite. The CEC of all soil layers is small in comparison to the cation charge of the landfill leachate. Therefore, adsorption will be limited.

The logic tree for site A with the probabilities assigned to the relevant branches is shown in Fig. 7 (above). Approximately 250 mm leachate per year seep into the subsoil of the landfill (Fig. 6). Approximately half of the leachate (125 mm/year) might reach the groundwater or surface water within a few hours to days due to fast macropore flow (step 2). Transport of the remaining solution (125 mm/year) will be retarded considerably due to the high pH value. The retention indicator would, for instance, be equal to 5.5 for Cd^{2+} and 7 for Cu^{2+} (step 3, step 3b can be omitted due to the small CEC). Therefore, the transport rate (velocity of pollutant front) according to Fig. 4 would approximately be 7 and 5.5 mm/year for Cd^{2+} and Cu^{2+} , respectively. The factor I (step 4) is $I = 400/125 = 3.2$. The groundwater table is more than 2 m below the surface (assumption 2–3 m, step 5). Therefore, the transport time of a hypothetical pollution front in the soil

Table 9
Model parameter settings and assumptions (European situation)

Parameter	Parameter value	Source
Surface area of Europe	7.16×10^6 km ²	[2]
Share of soil from surface area	48.5%	[2]
Storage density of soil	1500 kg/m ³	[38]
Thickness of upper-soil layer	300 mm	[24]
Average yearly precipitation	700 mm/year	[2]
Average rate of new groundwater formation	35 mm/year (5% of precipitation)	[52]
Macropore flow	10 mm/year	Assumption
Matrix flow	25 mm/year	Assumption

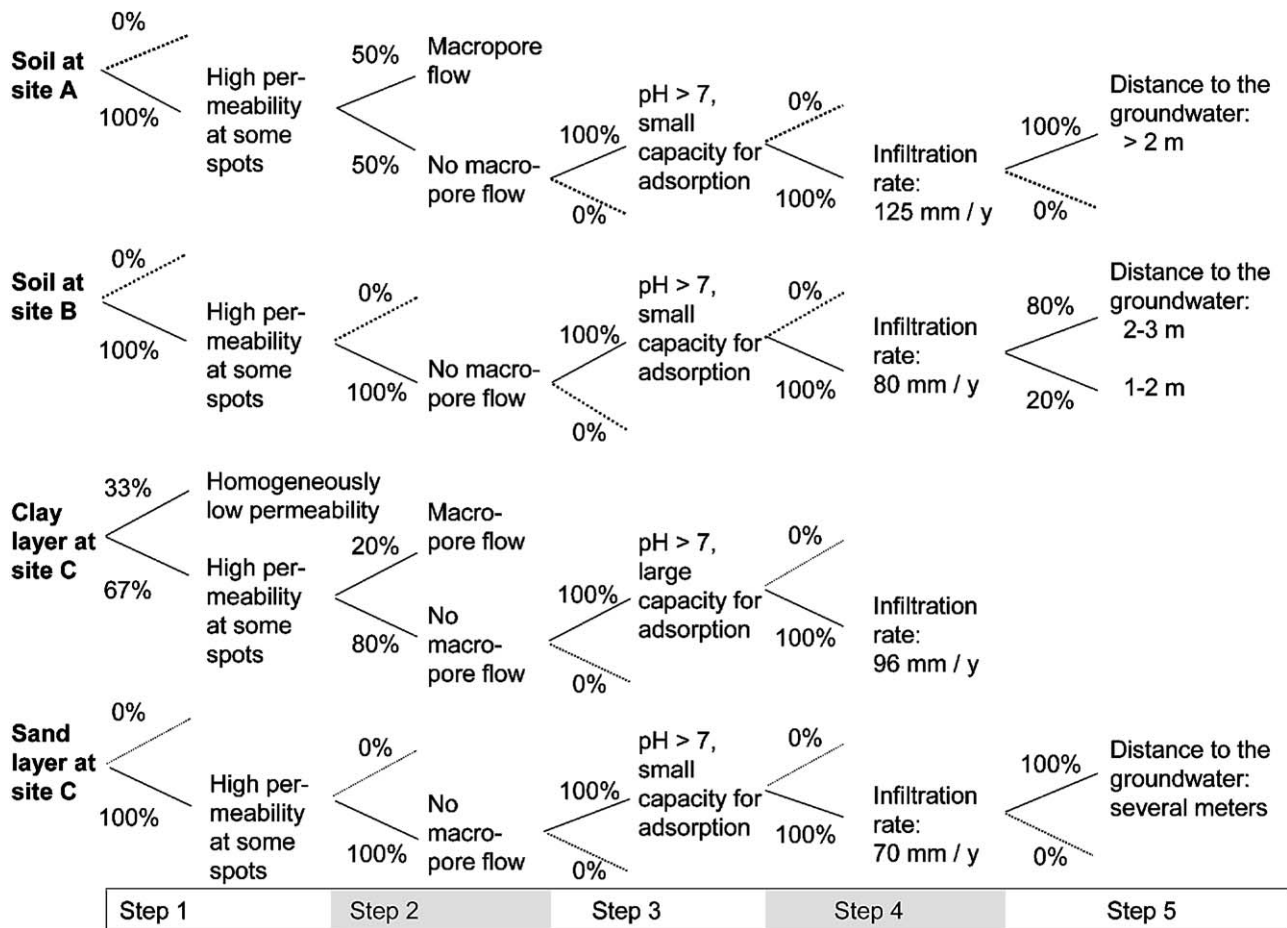


Fig. 7. Logic tree for sites A, B, and C. The branches carry the probabilities that are characteristic for these specific sites (see text). At site C, two logic trees are set up for two soil layers.

matrix can be estimated to be 910–1400 years for Cd^{2+} and 1200–1700 years for Cu^{2+} .

In summary, the geological barrier is rather weak at this site, since a large fraction of the leachate immediately reaches the groundwater through macropores. However, the leachate will be diluted considerably in the groundwater, thus preventing high concentrations.

4.2. Case study: site B

The bedrock (molasse) consists of marl (limy-clayey sediment) and sandstone (Fig. 8). This layer is heterogeneous, has many chasms and a hydraulic conductivity between 5×10^{-5} and 10^{-4} m/s (field test) due to the porous sandstone. The top moraine layer is between 1.4 and 7.1 m thick. It contains clayey areas with a hydraulic conductivity between 10^{-9} and 10^{-6} m/s as well as sandy areas with a hydraulic conductivity between 10^{-5} and 10^{-4} m/s [56,57]. It is assumed that the landfill leachate will flow through highly permeable sandy layers. Therefore, adsorption of heavy metals will be limited. Due to the high content of sand, the

probability for continuous macropore flow is small. Only 5.5% of the precipitation (55 mm/year) presently infiltrates into the moraine layer and leaches to the groundwater (Fig. 8). Since slag is more permeable than the moraine layer, we assume that more water would infiltrate into the landfill (assumption: 80 mm/year).

The groundwater table is lowered by a drainage system (2–3 m). In the long run, the drainage system might fail to work so that the water table might rise further. Dye tests revealed fast flow paths of the groundwater at the landfill site to several springs and the surface water [56,57]. The fraction of leachate flowing into the drinking water reservoir will be considerably diluted. However, concentrations in the water transported to the surface by springs might be high (the dilution ratio is approximately 1:2) [56,57].

The above information is summarized in the logic tree presented in Fig. 7 (2nd tree from above). All leaching water seeps into the subsoil matrix (steps 1 and 2). Due to the high pH value, the retention indicator would, for instance, be equal to 5.5 for Cd^{2+} and 7 for Cu^{2+} (step 3; step 3b can be omitted due to the small

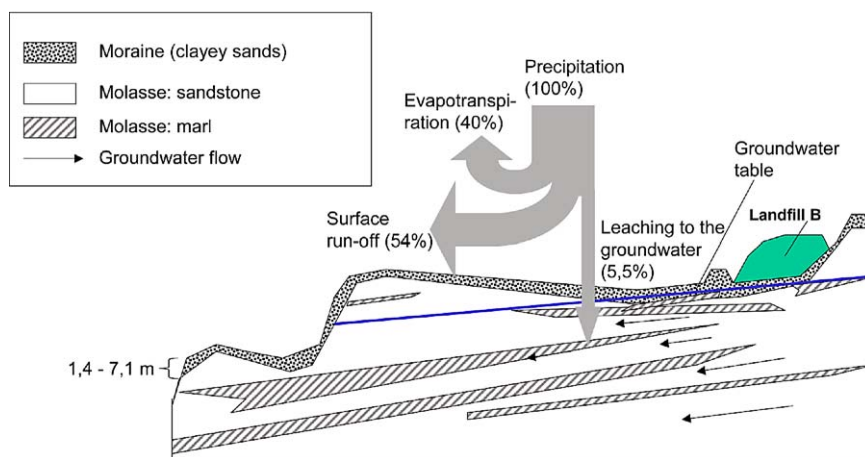


Fig. 8. Geological layers and water balance of site B [56,57]; only a small fraction of the rainwater (5.5%) seeps through the moraine layer to the groundwater. The groundwater table is high at this site (see line in the graph).

CEC). These indicator values correspond to transport rates of approximately 7 and 5.5 mm/year for Cd^{2+} and Cu^{2+} , respectively (Fig. 4). The total leaching from the landfill is 80 mm/year. Therefore, I is equal to $400/80 = 5$ (step 4). The distance to groundwater is assumed to be between 1 and 3 m (step 5). From here, the expected transport time for a potential pollution front to the groundwater table would be 710–2100 years for Cd^{2+} and 910–2700 years for Cu^{2+} . In contrast to site A, all heavy metals are retarded for at least 700 years. This time period might still be classified as short considering the long emission periods of landfills.

4.3. Case study: site C

At site C, it is planned to construct a landfill for grate incineration ash. The hydraulic conductivity of the rock material (molasse) is low (Fig. 9). The moraine contains gravel layers, which are 5–12 m thick. It is assumed that water circulation takes part in these zones [58,59]. Hydraulic connections to neighboring groundwater reservoirs have been identified [58]. In homogenous laboratory tests, the clay layer showed to have a hydraulic conductivity between 10^{-10} and 10^{-8} m/s [58]. However, in the field measurements k was between 1.6×10^{-7} and 3.6×10^{-6} m/s. Fig. 9 shows the water balance of the planned landfill before and after construction. The actual rate of new groundwater formation (10–20 mm/year) [58] is assumed to represent the leaching through the clay layer and the sea sediments to the gravel layers. Surface run-off and evapotranspiration are high due to the forest vegetation and the impermeable clay layers. Since slag is far more permeable, more water might infiltrate into the landfill though. The value of 18% proposed by Covelli [60] seems to be reasonable for a forest area. Since ponding conditions have been observed prior to landfill construction, it is assumed that only 12% of the rainwater may infiltrate

into the clay layer (120 mm/year). Therefore, part of the water (6% of precipitation, 60 mm/year) would flow away laterally on top of the clay layer. It is assumed that this fraction of leachate will flow into the surface water. Springs transport a large share of the leachate to the surface. It is assumed that only 7% of the initial amount of precipitation reaches the sea sediments and only 1–2% the groundwater.

In a risk analysis [60], the probability of macropore flow in the clay layer was estimated to be 20% (judgment of expert team). This value will be adopted in the present analysis. The probability of preferential flow in the sea sediments was estimated to be 0% [60] so that all the leachate flows through the soil matrix. The neutral to basic conditions would prevent any enhanced heavy metal concentrations due to precipitation/dissolution processes. Cation exchange further limits the mobility (the clay content varies between 5% and 40%).

Because the leachate seeps through the clay layer and the sea sediments before entering the groundwater, logic trees have to be established for both soil layers (Fig. 7, below). The leaching water from the landfill can only partially seep into the underlying clay layer (12% of precipitation, 120 mm/year). The rest (60 mm/year) flows into the surface water (step 1). A fraction of the seeping water (20%, 24 mm/year) flows through continuous macropores to the underlying sea sediments (step 2). The heavy metals contained in the remaining 80% matrix flow (96 mm/year) are subject to adsorption and possibly precipitation. Springs conduct 50 mm/year to the surface. For the remaining fraction (46 mm/year), the retention indicator (step 3a) would be 5.5 for Cd^{2+} and 7 for Cu^{2+} . Since the clay layer is thick, adsorption cannot be neglected. The supplements for the retention indicators according to step 3b would be between 0 and 1 for Cd^{2+} and between 0 and 2 for Cu^{2+} (clay content 5–40%, content of Fe-oxide unknown). The resulting transport rates according to Fig. 4 lie between 6 and

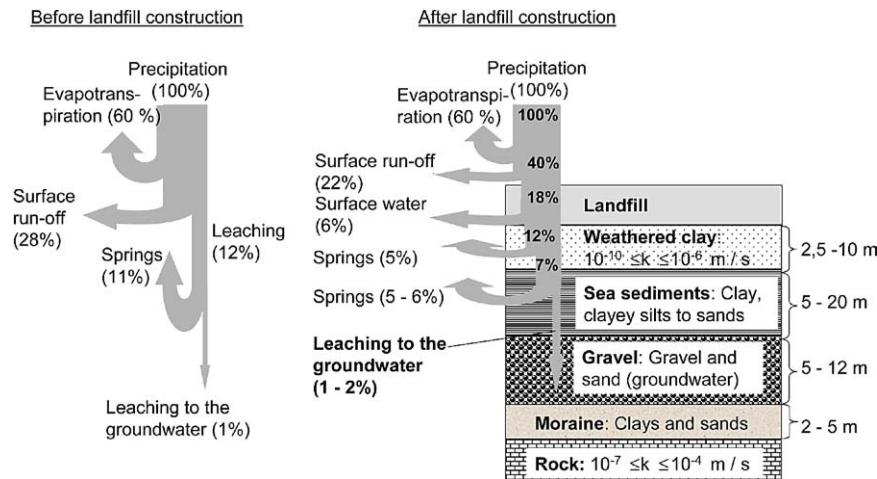


Fig. 9. Geological layers and water balance of a new landfill C prior to construction (left) and afterwards (right) (see text) [59].

7 mm/year for Cd^{2+} and between 3.5 and 5.5 mm/year for Cu^{2+} . The matrix infiltration rate into the clay layer was 96 mm/year, therefore I is equal to $400/96 = 4.1$ (step 4). Since the clay layer is between 2.5 and 10 m thick, it takes between 1500 and 6900 years for a potential Cd^{2+} -pollution front to reach the sea sediments and between 1900 and 12,000 years for Cu^{2+} .

All of the leaching water (70 mm/year) reaching the sea sediments seeps into this soil matrix (step 1 and 2). The retention indicators are 5.5 for Cd^{2+} and 7 for Cu^{2+} due to the high pH value (the transport rates are 7 and 5.5 mm/year for Cd^{2+} and Cu^{2+} , respectively). The capacity for adsorption is small; therefore, no supplements are given in step 3b. The infiltration rate into the sea sediments is 70 mm/year, therefore I is equal to $400/70 = 5.7$ (step 4). The distance to the groundwater is several meters (assumption: 5 m, step 5). A potential pollution of the groundwater could occur after further 4100 years for Cd^{2+} and 5200 years for Cu^{2+} .

According to the above analysis, the geological underground of this site works as an efficient barrier. Only a small fraction of the heavy metals reaches the groundwater (1–2%) and these heavy metals are significantly retarded. However, a large fraction of the leachate ends up in the surface water.

5. Multimedia-box-model calculations for Cd: results and discussion

The concentration increases of Cd in the compartments upper soil, deep soil, and groundwater were estimated with a simplified box model (Fig. 5), assuming an emission inflow of 1000 kg Cd to the upper-soil compartment (Section 3.2). The results of the simulation are shown in Table 10. They were calculated for different time horizons (similar to [2,51]). If the fraction of

macropore flow is assumed not to be polluted, concentrations in the groundwater remain unchanged during the first centuries after the emission inflow and start increasing thereafter. Steady state in the groundwater is only reached after a long time period (more than 10,000 years for Cd).

Our model could be integrated into existing LCIA methods that consider further inter-media transfer (e.g., from the fresh water to the sediments or to the seawater). For this purpose, we need to define rate constants for soil layers (vadose zone) and the groundwater. A rate constant a_{ij} accounts for exchanges of compartment i with other compartments j or, in case of $i=j$, for degradation (which is not relevant in the context of metals) [61]. Pollutants are transported from the upper-soil layer to the deeper soil layer, from there to the groundwater, and from there to the surface water (black arrows in Fig. 5). Therefore, we need to define three rate constants ($a_{\text{upper-soil,deep-soil}}$, $a_{\text{deep-soil,groundwater}}$, $a_{\text{groundwater,surface-water}}$). This can be done with the information obtained through the suggested procedure (Section 3.1). For instance, at the model site 'soil in Europe' (Table 8), the effective transport rate for Cd in the upper-soil layer $tr_{\text{upper-soil,eff}}$ was 0.44 mm/year ($tr_{\text{eff}} = tr_{400 \text{ mm}}/I$). The thickness of the upper-soil layer was assumed $d_{\text{upper-soil}} = 300$ mm. This gives a rate constant of $a_{\text{upper-soil,deep-soil}}$ of 0.00146 1/year ($a_{\text{upper-soil,deep-soil}} = tr_{\text{eff}}/d_{\text{upper-soil}}$). In Table 11, we suggest partitioning rate constants for the fictitious European site described in Table 8. These rate constants could directly be incorporated into existing multimedia-fate and exposure models, thereby allowing an assessment of emissions to deep soil layers and the groundwater. The results of the multimedia-model simulations are predicted concentrations in the environmental compartments considered and the PDI for humans. From here, risk ratios are calculated (see above). In current LCIA

Table 10

Results of the simulations of Cd transport through soil to the groundwater at a fictitious European site (lines 1–3), human exposure data (lines 4–5), and risk ratios for the groundwater (line 6). The inflow to the upper soil was assumed 1000 kg Cd/year. The values in the table are shown for time horizons of 20, 100, and 500 years and at steady state. In the calculation of the predicted daily intake (PDI, line 5), the daily intake of drinking water (WI) from groundwater was assumed to be $WI = 0.65\text{l/day}$ and the body weight 70 kg [2]

	Cd (non-polluted macropore flow)				Cd (polluted macropore flow, adequate for landfill emissions)			
	20 years	100 years	500 years	Infinite (steady state)	20 years	100 years	500 years	Infinite (steady state)
Concentration increase in the upper-soil layer (kg Cd/kg soil)	1.9×10^{-12}	7.0×10^{-12}	3.3×10^{-11}	4.4×10^{-11}	1.3×10^{-12}	4.9×10^{-12}	2.3×10^{-11}	3.1×10^{-11}
Concentration increase in the groundwater inflow (kg Cd/l)	0.0	0.0	0.0	8.2×10^{-6}	7.4×10^{-7}	7.4×10^{-7}	7.5×10^{-7}	8.2×10^{-6}
Concentrations in the groundwater $C_{\text{groundwater}}$ and the outflow to the fresh water (kg Cd/l) ^a	0.0	0.0	0.0	8.2×10^{-6}	2.1×10^{-7}	5.4×10^{-7}	7.4×10^{-7}	8.2×10^{-6}
Oral human limit value (HLV) [2] (kg/kg body weight/day)	1×10^{-9}	1×10^{-9}	1×10^{-9}	1×10^{-9}	1×10^{-9}	1×10^{-9}	1×10^{-9}	1×10^{-9}
Predicted daily intake (PDI) ^a of Cd from drinking water (groundwater pathway) (kg/kg body weight/day)	0	0	0	7.6×10^{-8}	2.0×10^{-9}	5.0×10^{-9}	6.9×10^{-9}	7.6×10^{-8}
Risk ratio = PDI/HLV	0	0	0	76	2.0	5.0	6.9	76

^a $PDI = WI \times C_{\text{groundwater}} / \text{body weight}$.

methods, these risk ratios are usually divided by the risk ratios of a reference substance in order to calculate toxicity potentials (e.g., [2]). If this reference substance is not a heavy metal, a similar procedure would need to be developed for the reference substance.

In the current work, we only illustrated the applicability of the method within current LCIA frameworks for one site. However, the site-dependent nature could also be used to either enable a more suitable assessment at a given site or to assess variability by considering ranges of possible values of all site parameters involved. An example of an extensive variability analysis with the help of a logic-tree approach is presented in [62].

6. Conclusions

The proposed procedure for estimating heavy metal transport in soil takes into account the most relevant processes (sorption, precipitation/dissolution, and surface complexation). However, there are still many open questions concerning the exact influence of these processes and other parameters that have not been discussed here, for instance, competition in heavy metal adsorption. It is difficult and often impossible to transform the specific knowledge of laboratory or field experiments into a generic procedure. One reason is that spatial parameters have an extremely high influence on the transport rates, but the exact field conditions at the landfill site are usually not known due to the heterogeneous nature of soils.

To maintain the methodology manageable, many simplifications were made. For instance, the mineral composition of the soil and the speciation of metals have only roughly been considered, because detailed information is impossible to obtain within the framework of an LCA. Further, the influence of temperature has been neglected. Moreover, the spatial parameters are assumed constant over time. A complete depletion of calcite and a subsequent drop of the pH value in the soil have not been taken into account. Although this scenario is not likely, because calcite comprises a significant fraction of Swiss soils at sites suitable for landfills, often greater than 30 wt% (in comparison, the calcite

content in the slag landfill is about 3.5% in average), it represents a possible long-term development.

The proposed procedure serves to estimate emission quantities. Moreover, it is possible to estimate averaged steady-state concentrations in the groundwater. Such concentrations at steady state are often used in the characterization step of toxic emissions in LCIA [2,49]. On the contrary, the prediction of actual concentrations reaching the groundwater is not directly possible within the current work. The fraction of the leachate flowing through macropores will probably not be diluted. However, the heavy metals flowing through the matrix are retarded in the soil. This effect could lower concentrations, but it could also enhance them as a consequence of accumulation with a subsequent local pH drop. The estimation of actual concentrations in the groundwater would further require information on groundwater conduits and further pollution sources. This information is usually not available. The inability of the methodology to directly predict actual concentrations in the groundwater makes the application of ‘above threshold approaches’ [13] difficult.

The validation of the proposed procedure is not feasible because of the long time horizons involved. However, measurements in the subsoil of landfills could give a first indication about the validity of the model. As heavy metals have probably not migrated much because of the relatively short history of slag landfills, other substances such as chlorides and sulfates would need to be used as indicators [63]. Another possibility of valuation is the application of the procedure to historical smelting sites and the comparison of the results to field measurements, as performed in Fig. 4. Unfortunately, the availability of large data sets is limited to a few studies [30,48].

The spatial characteristics considered in this work enable a site-dependent assessment of heavy metal emissions to the groundwater. If no information on specific characteristics is available, the suggested default values may be used for Swiss landfill sites. However, default values for other countries than Switzerland and other applications than landfills still need to be set up. The procedure may also be used to estimate the variability of possible transport times by defining

Table 11

Partitioning rate constants for Cd at a European model site (Table 8). These rate constants could be directly integrated into existing multimedia models

	Upper soil–deep soil	Deep soil–groundwater	Groundwater–surface water
Effective transport rate ^a (Columns 1 and 2) or outflow from the groundwater (Column 3)	0.44 mm/year	0.47 mm/year	120,000,000 l
Distance <i>d</i> (Columns 1 and 2) or groundwater volume GW volume (Column 3)	300 mm	200–4700 mm	1,200,000,000 l
Partitioning rate constant <i>a</i> ^b	0.00146 y ⁻¹	0.0000997–0.00234 y ⁻¹	0.1 y ⁻¹

^a $tr_{\text{eff}} = tr_{\text{Table8}}/I_{\text{Table8}}$.

^b $a = tr_{\text{eff}}/d$ or $a = \text{outflow}/\text{GW volume}$.

ranges instead of exact values of some parameters as input, e.g., if some of the spatial information is not available.

The proposed generic procedure serves to classify the mobility of heavy metal cations in a given soil. Thereby, we offer an alternative to neglecting the emissions to the deeper soil layers and the groundwater. This neglect is, in our opinion, not consistent with the life-cycle approach since all emissions from cradle to grave should be considered. Heavy metal emissions to deeper soil layers have important environmental impacts concerning processes such as waste treatment if long-term time horizons are considered and should therefore not be disregarded [10]. In this sense, we think that our procedure is a good starting point for further developments.

The method proposed in this paper calculates when impacts are to be expected from a certain emission and, therefore, the unit of the model outcome is ‘time’. This information may be useful in some applications. For instance, instead of simply neglecting emissions to the deep soil and the groundwater we now have the option of considering or neglecting them by considering the time when they occur. Alternatively, explicit discounting (temporal cut-offs are a special case of discounting) could be applied as demonstrated in [17]. However, processing temporal information in LCA as obtained by the application of our guidelines is a new research area and has only been applied in few case studies so far [17]. Therefore, we needed to adapt the method to make it compatible to existing LCIA methods. In Section 5, we gave an example of how our procedure may be integrated into an existing LCIA multimedia-fate and exposure model. The risk ratios calculated there for human exposure are compatible with other LCIA methods [2], but they would need to be divided by the risk ratios of a reference substance. If this reference substance is not a heavy metal (e.g., 1,4-dichlorobenzene in the case of USES-LCA [64]), a similar approach assessing transport through soil to the groundwater would need to be defined for this substance.

While some information is lost in the box-model approach (e.g., the temporal resolution in case of steady-state modeling) it may be a step towards improving the modeling of the groundwater compartment in current multimedia-fate models. One major advantage of our method would be that the assessment can easily be adapted to a given site and that uncertainties due to spatial variability could be assessed.

Acknowledgements

We thank Prof. Rainer Schulin for his comments and support in the development of the method. We are also grateful to Dr. Markus Leuenberger and Dr. Bruno

Covelli for providing the data of the case studies, Dr. Eddi Höhn for taking time to explain us some basics about geology, and Max Stroebe for mathematical support. The funding of the project by the Swiss National Science Foundation within the Swiss Priority Program Environment (SPPE) is gratefully acknowledged.

References

- [1] Goedkoop M, et al. The eco-indicator 99: a damage oriented method for life cycle impact assessment. Methodology Report, Amersfoort: Pré Consultants; 1999.
- [2] Huijbregts MAJ. Priority assessment of toxic substances in the frame of LCA. Amsterdam: University of Amsterdam (NL); 1999.
- [3] SAEFL. Bewertung in Ökobilanzen mit der Methode der ökologischen Knappheit. Ökofaktoren 1997. SRU-297, Bern: Swiss Agency for the Environment, Forests and Landscape; 1998.
- [4] Hauschild M, Wenzel H. Environmental assessment of products; scientific background. London: Chapman & Hall; 1997.
- [5] Goedkoop M. The eco-indicator 95—weighting method for environmental effects that damage ecosystems or human health on a European scale. Amersfoort: Novem; 1995.
- [6] Heijungs R, Guinee J, Huppes G, Lankreijer RM, Udo de Haes HA, Wegener-Sleeswijk A. Environmental life cycle assessment of products. Leiden: CML; 1992.
- [7] Steen B. A systematic approach to environmental priority strategies in product development (EPS). Version 2000—general system characteristics. Stockholm (S): Centre for Environmental Assessment of Products and Material System; Chalmers University of Technology; 1999.
- [8] Parkhurst DL, Appelo CAJ. Users Guide to PHREEQC (V2)—A computer program for speciation, batch-reaction, one-dimensional transport, and inverse geochemical calculations. Water-Resources Investigation Report, 99-4259. Denver: US Geological Survey; 1999.
- [9] SAEFL. Two-dimensional flow and transport in unsaturated soils. Environmental Series, SRU 259-e. Bern: Swiss Agency for the Environment, Forests and Landscape; 1996.
- [10] Hellweg S, Doka G, Finnveden G, Hungerbühler K. Waste and ecology: which technologies perform best?. In: Ludwig C, Hellweg S, Stucki S, editors. Municipal solid waste management: strategies and technologies for sustainable solutions. Berlin, Heidelberg, New York: Springer; 2003. p. 350–404.
- [11] Owens JW. LCA impact assessment categories. *Int J LCA* 1996; 1(3):151–8.
- [12] Potting J, Hauschild M. Predicted environmental impact and expected occurrence of actual environmental impact: the linear nature of environmental impact from emissions in life-cycle assessment. *Int J LCA* 1997;2(3):171–7.
- [13] Potting J, Hauschild M, Wenzel H. “Less is Better” and “Only Above Threshold”: two incompatible paradigms for human toxicity in life cycle assessment? *Int J LCA* 1999;4(1):16–24.
- [14] Potting J, Schöpp W, Blok K, Hauschild M. Site-dependent life-cycle impact assessment of acidification. *J Ind Ecol* 1998;2(2): 63–87.
- [15] Tolle DA. Regional scaling and normalization in LCIA. *Int J LCA* 1997;2(4):197–208.
- [16] Finnveden G. Valuation methods within LCA—where are the values. *Int J LCA* 1997;2(3):163–9.
- [17] Hellweg S, Hofstetter TB, Hungerbühler K. Discounting and the environment: should current impacts be weighted differently than impacts harming future generations?. *Int J LCA* 2003;8(1):8–18.

- [18] Norris GA. Integrating life cycle cost analysis and LCA. *Int J LCA* 2001;6(2):118–20.
- [19] van Beukering P, Oosterhuis F, Spaninks F. Economic valuation in life cycle assessment. Applied to Recycling and Solid Waste Management. Working Paper, W98/02. Amsterdam: Institute for Environmental Studies, Vrije Universiteit; 1998.
- [20] Hellweg S, Hofstetter TB, Hungerbühler K. Time-dependent life-cycle assessment of emissions from slag landfills with the help of scenario analysis. *J Cleaner Prod* (accepted for publication).
- [21] Leuenberger M. Beurteilung Endlagersicherheit (>100 Jahre): Überlegungen zur Langzeitstabilität und zur Prognosesicherheit. Working Paper. Münsingen: Rytec; 1997.
- [22] Hermanns-Stengele R. Personal communication. Institut für Geotechnik, ETH Zurich, 1999.
- [23] Baccini P, Belevi H, Lichtensteiger T. Die Deponie in einer ökologisch orientierten Volkswirtschaft. *GAIA* 1992;1(1):34–49.
- [24] Deutscher Verband für Wasserwirtschaft und Kulturbau. Filtereigenschaften des Bodens gegenüber Schadstoffen. 212, Hamburg, Berlin, 1988.
- [25] Schweizerische Bundesrat. Verordnung über die Umweltverträglichkeit. Bern, 1988.
- [26] Stauffer F. Personal communication. Institut für Hydromechanik und Wasserwirtschaft, ETH Zurich, 2000.
- [27] Flury M. Transport of bromide and chloride in a sandy and a loamy field soil. PhD Thesis, Universität Zurich, No. 10185, Zurich, 1993.
- [28] Beven K, Germann PF. Macropores and water flow in soil. *Water Resource Res* 1982;18(5):1311–25.
- [29] Cernik M, Federer P, Borkovec M, Sticher H. Modeling of heavy metal transport in a contaminated soil. *J Environ Quality* 1994; 23:1239–48.
- [30] Maskall J, Whitehead K, Thornton I. Heavy metal migration in soils and rocks at historical smelting sites. *Environ Geochem Health* 1995;17:127–38.
- [31] Sidle RC, Kardos LT. Transport of heavy metals in a sludge-treated forested area. *J Environ Quality* 1977;6:431–7.
- [32] Richards BK, Steenhuis TS, Pevery JH, McBride MB. Metal mobility at an old, heavily loaded sludge application site. *Environ Pollut* 1998;99:365–77.
- [33] Cambreco VJ, Richards BK, Steenhuis TS, Pevery JH, McBride MB. Movement of heavy metals through undisturbed and homogenized soil columns. *Soil Sci* 1996;161(11):740–50.
- [34] Iqbal MZ. Role of macropores in solute transport under ponded water condition produced by laboratory simulated intense storms. *Ground Water* 1999;37(5):674–81.
- [35] Boontink HWG, Bouma J. Sensitivity analysis on processes affecting bypass flow. *Hydrological Processes* 1993;7:33–43.
- [36] Scheffler F, Schachtschabel P. Lehrbuch der Bodenkunde. Stuttgart: Enke; 1998.
- [37] Kessler JH, McGuire RK. Total system performance assessment for waste disposal using a logic tree approach. *Risk Anal* 1999; 19(5):915–31.
- [38] Schulin R. Personal communication. Institut für Terrestrische Ökologie, ETH Zurich, 2000.
- [39] Schweizerischer Bundesrat. Technische Verordnung über Abfälle (TVA). Bern: Schweizerischer Bundesrat; 1990.
- [40] Djodjic F, Berström L, Ulen B, Shirmohammadi A. Mode of transport of surface-applied phosphorus-33 through a clay and sandy soil. *J Environ Quality* 1999;28(4):1273–82.
- [41] Bergström LF, Shirmohammadi A. Areal extent of preferential flow with profile depth in sand and clay monoliths. *J Soil Contam* 1999;8(6):637–51.
- [42] Germann PF, Edwards WM, Owens LB. Profiles of bromide and increased soil moisture after infiltration into soils with macropores. *Soil Sci Soc Amer J* 1984;48:237–45.
- [43] Höhn E. Personal communication. Dübendorf (CH): EAWAG, 1999.
- [44] Hellweg S, Hotstetter TB, Hungerbühler K. Modeling waste incineration for life cycle inventory analysis in Switzerland. *Environ Model Assess* 2001;6(4):219–35.
- [45] Plüss A. Charakterisierung von Rauchgasreinigungsrückständen aus Müllverbrennungsanlagen und deren Immobilisierung mit Tonmineralien. Zurich, v/d/f, 1993.
- [46] Johnson A. Chemische Eigenschaften und Langzeitverhalten der Müllschlacke. In: Baccini P, Gamper B, editors. Deponierung fester Rückstände aus der Abfallwirtschaft. Zurich, v/d/f; 1993. p. 35–54.
- [47] Zimmermann P, Doka G, Huber F, Labhardt A, Menard M. Ökoinventare von Entsorgungsprozessen, Grundlagen zur Integration der Entsorgung in Ökobilanzen. ESU-Reihe, 1/96, Zurich: Institut für Energietechnik, ETH Zurich; 1996.
- [48] Maskall J, Whitehead K, Gee C, Thornton I. Long-term migration of metals at historical smelting sites. *Appl Geochem* 1996;11:43–51.
- [49] Hertwich EG, Mateles SF, Pease WS, Mckone TE. Human toxicity potentials for life-cycle assessment and toxics; release inventory risk screening. *Environ Toxicol Chem* 2001;20(4):928–39.
- [50] Mackay D, Guardo AD, Paterson S, Kicsi G, Cowan CE. Assessing the fate of new and existing chemicals: a five stage process. *Environ Toxicol Chem* 1996;15(9):1618–26.
- [51] Huijbregts MAJ, Guinée JB, Reijnders L. Priority assessment of toxic substances in the frame of LCA. III: export of potential impact over time and space. *Chemosphere* 2001;44:59–65.
- [52] McKone TE, Bodnar AB, Hertwich EG. Development and evaluation of state-specific landscape data sets for multimedia source-to-dose models. Berkeley: School of Public Health, University of California; 2001 LBNL-43722.
- [53] Martinson C. Geochemical interactions of a saline leachate with molasse at a landfill site: a case study. *Ecolgae Geol Helv* 1994; 87(2):473–86.
- [54] Rytec. Fallbeispiel A: Situationsanalyse, Risikobeurteilung Sicherstellung der Nachsorge. Münsingen; 1997.
- [55] Rytec. Fallbeispiel A: Synthesebericht. Münsingen; 1998.
- [56] Rytec. Fallbeispiel B: Geologie, Hydrogeologie, Standortqualität, Anforderungen Deponiesystem. Münsingen; 1998.
- [57] Rytec. Fallbeispiel B: Risikoabschätzung. Münsingen; 1998.
- [58] Buser&Finger. Deponie Oberholz, Suhr: Bericht zur Umweltverträglichkeit, Stufe 2. Internal Report, Zurich: Baudepartement des Kantons Aargau, 1997.
- [59] Eberhard. Deponie Oberholz: Geologisch-Hydrogeologische und Geotechnische Untersuchungen. Internal Report, Aarau: Baudepartement des Kantons Aargau, 1995.
- [60] Covelli B. Langzeitbewertung der Grundwassergefährdung in der geplanten Deponie Oberholz. Internal Report. Lentzburg, 1995.
- [61] Trapp S, Matthies M. Chemodynamics and environmental modeling: an introduction. Berlin, Heidelberg, New York: Springer; 1997.
- [62] Geisler G, Hellweg S, Hungerbühler K. Assessing groundwater exposure to pesticides in LCA considering spatial and temporal variability. Submitted to Environmental Science and Technology.
- [63] Kräuchi P, Gubler R. Kehrichtschlacke als Strassenbaumaterial. Diploma Thesis, ETH Zurich, 1992.
- [64] Huijbregts MAJ. Priority assessment of toxic substances in the frame of LCA—the multi-media fate, exposure and effect model USES-LCA. Amsterdam: University of Amsterdam (NL); 1999.
- [65] Li Y, Ghodrati M. Preferential transport of solute through soil columns containing constructed macropores. *Soil Sci Soc Amer J* 1997;61:1308–17.
- [66] Ghodrati M, Chendorain M, Chang YJ. Characterization of macropore flow mechanisms in soil by means of a split macropore column. *Soil Sci Soc Amer J* 1999;63:1093–101.
- [67] Oostindie K, Bronswijk JJB. Consequences of preferential flow in cracking clay soils for contamination-risk of shallow aquifers. *J Environ Manage* 1995;43:359–73.

- [68] Germann PF. Rapid drainage response to precipitation. *Hydrol Processes* 1986;1:3–13.
- [69] Bouma J, Dekker LWA. Case study on infiltration into dry clay soil: I. morphological observations. *Geoderma* 1978;20:27–40.
- [70] Bronswijk JJB. Modeling of water balance, cracking and subsidence of clay soils. *J Hydrol* 1988;97:199–212.
- [71] Pruss K. On water seepage and fast preferential flow in heterogeneous, unsaturated rock fractures. *J Contam Hydrol* 1998;30:333–62.
- [72] Bourg ACM. Metals in aquatic and terrestrial systems: sorption, speciation, and mobilization. In: Salomons W, Förster U, editors. *Chemistry and biology of solid waste*: Springer; 1988. p. 3–32.
- [73] van Stiphout TPJ, van Lanen HAJ, Boersma OH, Bouma J. The effect of bypass flow and internal catchment of rain on the water regime in a clay loam grassland soil. *J Hydrol* 1987;95: 1–11.
- [74] Jorgensen PR, Schroder T. Validation and development of pesticide leaching models. 47, Ministry of Environment and Energy, Danish Environmental Protection Agency; 1998.
- [75] Hendriks RFA, Oostindie K, Hamminga P. Simulation of bromide tracer and nitrogen transport in a cracked clay soil with the FLOCR/ANIMO Model combination. *J Hydrol* 1999;215:94–115.
- [76] Wilkison DH, Blevins DW. Observations on preferential flow and horizontal transport of nitrogen fertilizer in the unsaturated zone. *J Environ Quality* 1999;28:1568–80.
- [77] Bronswijk JJB, Hamminga W, Oostindie K. Rapid nutrient leaching to groundwater and surface water in clay soil areas. *Eur J Agron* 1995;4(4):431–9.
- [78] Bronswijk JJB, Hamminga W, Oostindie K. Field-scale solute transport in a heavy clay soil. *Water Resources Res* 1995;31(3): 517–26.
- [79] Munsell Soil Color Charts. Available from: http://www.drcrow.org/_f2003%20FS/munsell.html. Internet, 2003.